Electronic Supporting Information for

Violet-Emitting Distributed-Feedback Laser using a Naphtho[2,1-*b*:6,5-*b*']difuran Derivative

Hayato Tsuji,*[a] Akihiro Shitomi,[a] Naoto Hamaguchi,a Yasunobu Egawa,[a] Víctor Bonal,[b] Pedro G. Boj,[c] José M. Villalvilla,[b] José A. Quintana,[c] and María A. Díaz-García *[b]

[a] *Department of Chemistry, Faculty of Science, Kanagawa University, Tsuchiya 2946, Hiratsuka 259-1293, Japan.*

[b] *Dpto. Física Aplicada and Instituto Universitario de Materiales de Alicante (IUMA), Universidad de Alicante, Alicante 03080, Spain.*

[c] *Dpto. Óptica, Farmacología y Anatomía and IUMA, Universidad de Alicante, Alicante 03080, Spain.*

1. General experimental details and methods

1.1. Sample preparation

Active thin films based on PS (Merck, M_W = 35,000 g mol^{-1}) doped with **C8-DPNDF**, between 0.1 to 6 wt%, were spin-coated at 3000 rpm on FS substrates (25 × 25 × 1 mm) using toluene as solvent. The percentage of PS in the solvent was adjusted to obtain proper thickness for the films, so they constituted waveguides supporting only fundamental transversal modes with a high confinement factor (Γ~90%). This helps to minimize losses, and thus to optimize the ASE performance.[1,2] Film thickness was measured using a spectrophotometric method previously reported.[3] The uniformity and optical quality of active film waveguides is very high as can be shown by the observation of well-resolved interference fringes in the transparent window of optical absorption spectrum of the film, and their coincidence with theoretical predictions.[4]

The DFB laser architecture consists of a dichromated gelatin (DCG) resonator on top of the active film. The fabrication procedure is described in detail in previous publications.[5,6] Main steps are as follows: i) A water solution of gelatin (Rousselot 200 bloom) sensitized with ammonium dichromate is spin-coated on top of the active film; ii) A 1D grating is recorded by holographic lithography using the Lloyd configuration with light from an Ar laser emitting at 364 nm; iii) A final surface relief grating is obtained, after desensitization, by dry-develop in an oxygen plasma. The device is prepared to operate in the second order of diffraction, which means m = 2 in the Bragg condition:

$$m\,\lambda_{Bragg} = 2\,n_{eff}\,\Lambda \qquad (1)$$

where n_{eff} is the effective refractive index of the waveguide and Λ is the grating period. Thus, the emission wavelength for each device can be varied by selecting the grating period, as can be seen in Table 2 of the main text.

1.2. Optical characterization

Absorption and photoluminescence measurements of active films were made with a double-beam Jasco V-650 spectrophotometer and a Jasco FP-6500 spectrofluorometer, respectively. ASE and DFB laser characterization were made using a Nd:YAG pulsed laser operating at 355 nm, with a repetition rate of 10 Hz and a pulse duration of 10 ns. ASE characterization was made by exciting the active film at normal incidence with a 3.5 × 0.5 mm stripe beam and collecting the output light from the edge of the film. In the case of DFB lasers, the devices were illuminated at a 30° angle with a circular beam, and the emitted light was collected perpendicularly to the film plane. Both types of measurements were made using an Ocean Optics USB2000 UV-Vis spectrometer with a resolution of 0.6 nm.

2. Details on the ASE experiments

In this section, we provide details on the experiments conducted to study the ASE properties discussed in the manuscript. The ASE parameters obtained for the various films (emission wavelength, emission linewidth, threshold and operational lifetime) have been collected in Table 1 of the main manuscript. To illustrate how these parameters are obtained, we show in Figure S1 data for the film doped with 0.25wt% (Figures S1 a,b,c). For this film, gain coefficients at different pump density energies and losses have also been determined (Figure S1d).

a)

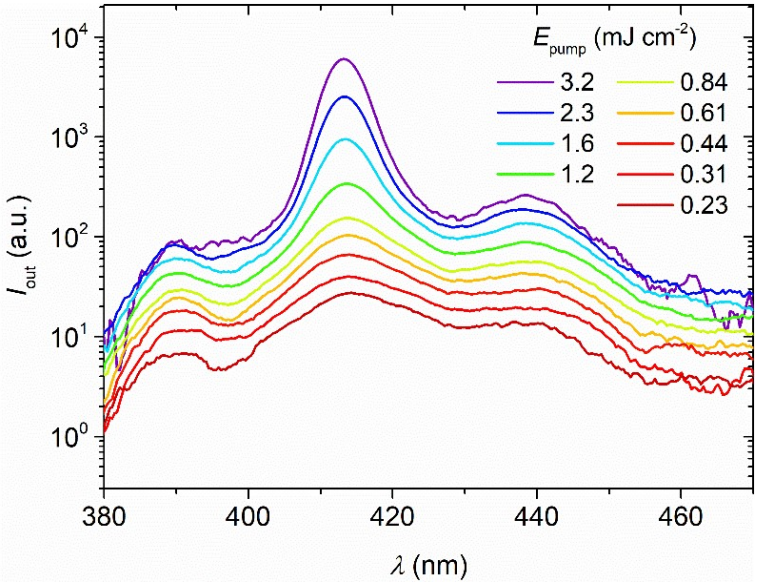

b)

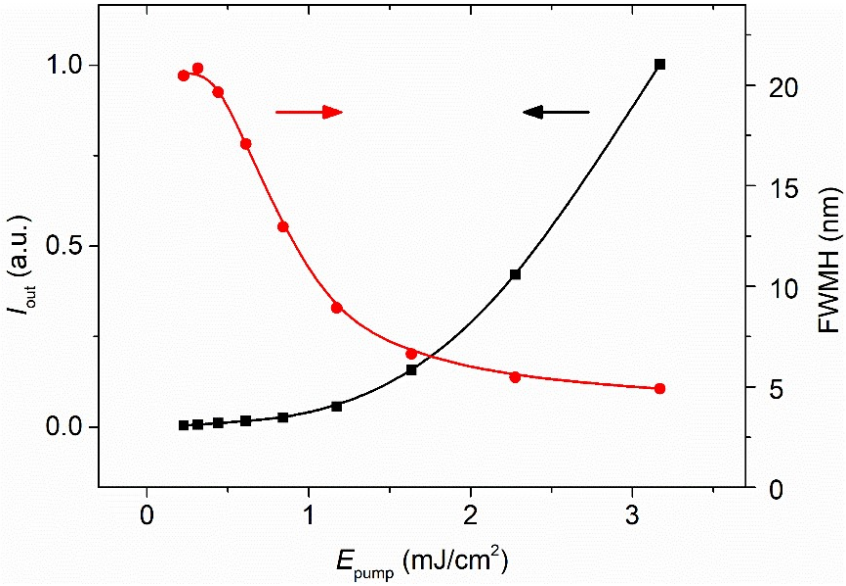

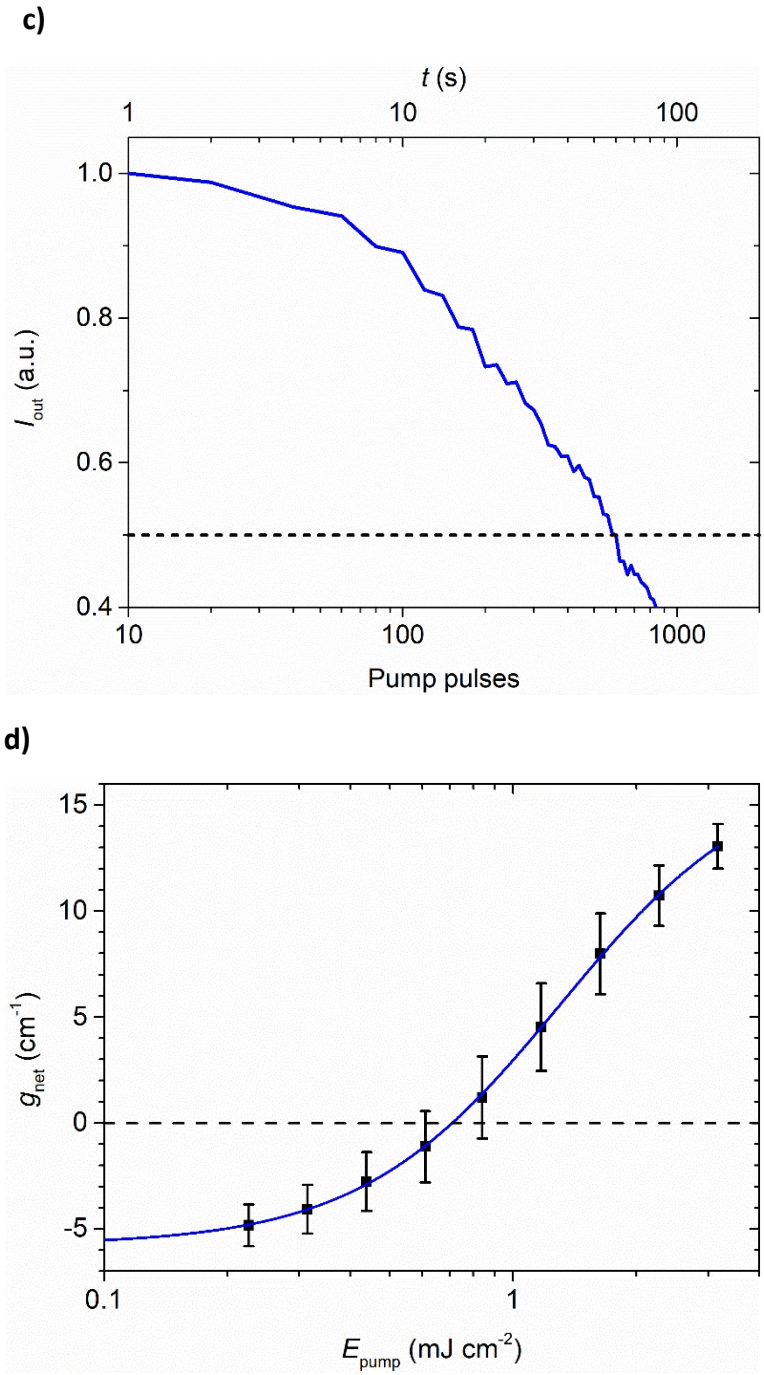

Figure S1. ASE characterization of PS films containing 0.25 wt% of C8-DPNDF. a) Emission spectra at different pump energy densities, E_{pump} (see legend); b) Output intensity at the wavelength at which ASE appears, I_{out}, (black squares, left axis) and emission linewidth, FWHM, (red circles, right axis) as a function of E_{pump},. Full lines are guides to the eye. The ASE threshold value was determined from the FWHM versus the E_{pump} plot as the E_{pump} value at which FWHM decays to half of its maximum value. This value approximately coincides with that at which a drastic change in the slope of the I_{out} versus the E_{pump} curve occurs.; c) ASE intensity, I_{out}, versus the number of pump pulses and time (bottom and top axes, respectively) with E_{pump} = 2.2 mJ/cm^2 (two times

higher than the threshold). The operational ASE lifetime ($\tau_{ASE}^{1/2}$) is defined as the time (or number of pump pulses), at which I_{out} decays to half of its initial value; d) Net gain coefficients, g_{net}, at the ASE peak wavelength versus E_{pump}, The full line is a guide to the eye and its intersection with the y-axis corresponds to the loss coefficient (α = 5 ± 1 cm^{-1}). The g_{net} values were obtained with a method reported by. Cerdán et al,[7,8] based on the analysis of a series of emission spectra at different E_{pump} values.

3. Comparison of the C8-DPNDF ASE and laser performance to that of other materials

In this section we compare, first, the ASE threshold performance of **C8-DPNDF** dispersed in PS films to that of other dyes dispersed in PS (Figure S2). For a meaningful comparison, the absorption coefficient, which depends on the dye-doping rate in the film, has been taken into account. The materials considered in the comparison have ASE wavelengths in the same spectral range.

Secondly, we compare the DFB performance of the C8-DPNDF devices prepared in this work, to that of other DFB lasers based on other materials (Table S1).

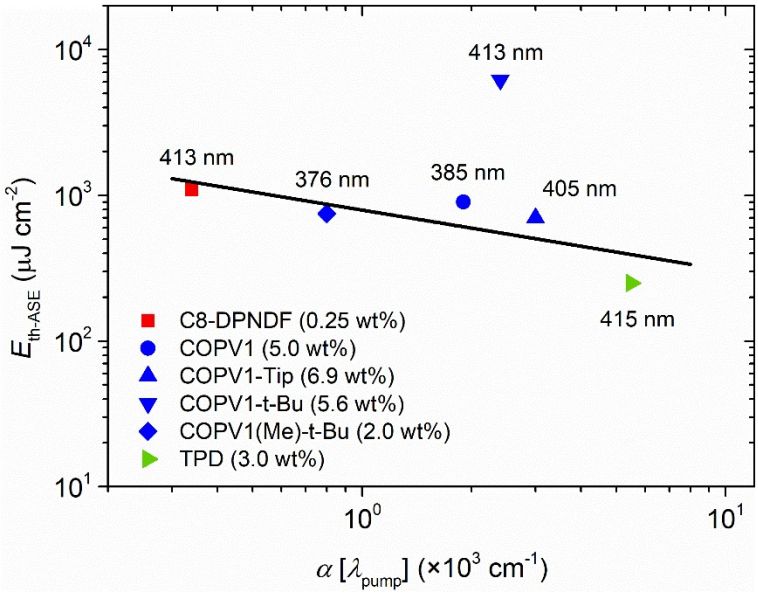

Figure S2. Amplified spontaneous emission threshold comparison. ASE thresholds, $E_{th\text{-}ASE}$, versus the absorption coefficient at the pump wavelength, $\alpha[\lambda_{pump}]$, for PS films doped with different small molecules previously studied.[6,9] The full line is a guide to the eye to show the behavior trend for most of the compounds. The compounds selected in the comparison have ASE wavelengths in the same spectral region (values for each compound shown next to its corresponding symbol in the figure).

Table S1. Comparison of DFB lasers emitting in the violet spectral range. Grating materials include dichromated gelatin (DCG) and silicon dioxide (SiO_2). The different techniques used to fabricate the grating are holographic lithography (HL) and electron- beam lithography (EBL). The reference marked with an asterisk (*) corresponds to the present work.

Material	Concentration	Grating material	Grating fabrication	λ_{pump} (nm)	α [λ_{pump}] ($\times 10^3$ cm^{-1})	λ_{ASE} (nm)	$E_{th\text{-}ASE}$ (μJ cm^{-2})	λ_{DFB} (nm)	$E_{th\text{-}DFB}$ (μJ cm^{-2})	Reference
C8-DPNDF	0.25 wt% in PS	DCG	HL	355 (10 ns, 10 Hz)	0.34	413	1100	411-417	2000	*
COPV1	5.0 wt% in PS	DCG	HL	355 (10 ns, 10 Hz)	1.9	385	900	383-396	2000	[9,10]
COPV1-Tip	6.9 wt% in PS	DCG	HL	355 (10 ns, 10 Hz)	3.0	405	700	402-416	900	[9,10]
COPV1-*t*-Bu	5.6 wt% in PS	DCG	HL	355 (10 ns, 10 Hz)	2.4	413	6200	409-421	1200	[9,10]
COPV1(Me)-*t*-Bu	2.0 wt% in PS	DCG	HL	355 (10 ns, 10 Hz)	0.80	376	750	375-385	1000	[10]
TPD	3.0 wt% in PS	DCG	HL	355 (10 ns, 10 Hz)	5.5	415	250	420	400	[6,11]
TDAF-1	Neat	SiO_2	EBL	355 (10 ns, 10 Hz)	-	430	7	423	5.3	[12,13]
H-CH_3	Neat	SiO_2	-	355 (300 ps, 23 Hz)	41	423	10.7	412	45	[14]

4. References

1 R. Muñoz-Mármol, N. Zink-Lorre, J. M. Villalvilla, P. G. Boj, J. A. Quintana, C. Vázquez, A. Anderson, M. J. Gordon, A. Sastre-Santos, F. Fernández-Lázaro and M. A. Díaz-García, *J. Phys. Chem. C*, 2018, **122**, 24896–24906.

2 M. G. Ramírez, M. Morales-Vidal, V. Navarro-Fuster, P. G. Boj, J. A. Quintana, J. M. Villalvilla, A. Retolaza, S. Merino and M. A. Díaz-García, *J. Mater. Chem. C*, 2013, **1**, 1182–1191.

3 V. Bonal, J. A. Quintana, J. M. Villalvilla, R. Muñoz-Mármol, J. C. Mira-Martínez, P. G. Boj, M. E. Cruz, Y. Castro and M. A. Díaz-García, *Polymers (Basel).*, 2021, **13**, 2545.

4 V. Bonal, J. A. Quintana, R. Muñoz-Mármol, J. M. Villalvilla, P. G. Boj and M. A. Díaz-García, *Thin Solid Films*, 2019, **692**, 137580.

5 J. A. Quintana, J. M. Villalvilla, M. Morales-Vidal, P. G. Boj, X. Zhu, N. Ruangsupapichat, H. Tsuji, E. Nakamura and M. A. Díaz-García, *Adv. Opt. Mater.*, 2017, **5**, 1700238.

6 V. Bonal, J. A. Quintana, J. M. Villalvilla, P. G. Boj, R. Muñoz-Mármol, J. C. Mira-Martínez and M. A. Díaz-García, *Polymers (Basel).*, 2021, **13**, 3843.

7 L. Cerdán, *Opt. Laser Technol.*, , DOI:10.1016/j.optlastec.2019.105814.

8 L. Cerdán, M. Anni, M. L. De Giorgi, P. G. Boj and M. A. Díaz-García, *Opt. Laser Technol.*, 2021, **136**, 106766.

9 V. Bonal, M. Morales-Vidal, P. G. Boj, J. M. Villalvilla, J. A. Quintana, N. Lin, S. Watanabe, H. Tsuji, E. Nakamura and M. A. Díaz-García, *Bull. Chem. Soc. Jpn.*, 2020, **93**, 751–758.

10 V. Bonal, J. M. Villalvilla, J. A. Quintana, P. G. Boj, N. Lin, S. Watanabe, K. Kazlauskas, O. Adomeniene, S. Jursenas, H. Tsuji, E. Nakamura and M. A. Díaz-García, *Adv. Opt. Mater.*, 2020, **8**, 2001153.

11 E. M. Calzado, J. M. Villalvilla, P. G. Boj, J. A. Quintana and M. A. Díaz-García, *Org. Electron.*, 2006, **7**, 319–329.

12 H. W. Lin, C. L. Lin, C. C. Wu, T. C. Chao and K. T. Wong, *Org. Electron.*, 2007, **8**, 189–197.

13 W. Huang, S. Shen, D. Pu, G. Wei, Y. Ye, C. Peng and L. Chen, *J. Phys. D. Appl. Phys.*, 2015, **48**, 495105.

14 Y. Qian, Q. Wei, G. Del Pozo, M. M. Mrõz, L. Lüer, S. Casado, J. Cabanillas-Gonzalez, Q. Zhang, L. Xie, R. Xia and W. Huang, *Adv. Mater.*, 2014, **26**, 2937–2942.